Thermal Stability of Surfactants with Amino and Imido Groups in Poly(Ethylene Terephthalate)/Clay Composites

Xuepei Yuan, Chuncheng Li, Guohu Guan, Yaonan Xiao, Dong Zhang

CAS Key Laboratory of Engineering Plastics, Joint Laboratory of Polymer Science and Materials, Center for Molecular Science, Institute of Chemistry, Chinese Academy of Sciences, Beijing 100080, People's Republic of China

Received 4 June 2007; accepted 19 March 2008
DOI 10.1002/app.28431
Published online 11 June 2008 in Wiley InterScience (www.interscience.wiley.com).

ABSTRACT: Effects of thermal stability of surfactants with amino and imido groups on thermal properties of poly(ethylene terephthalate) (PET)/clay composites were studied. The imidosilane surfactant was synthesized successfully from the imide reaction between amino silane and phthalic anhydride. TGA shows that imidosilane decomposition behaviors have two major stages according to the degradations of different functional groups. After melt extrusion, the decomposition of amino functional groups in amino surfactants decreases the thermal stability of organoclay and accelerates the degradation behaviors of PET composites. Because of the enhanced thermal stability of imidosilane surfactants, PET/imido-palygorskite (PT) composites represent enhanced thermal stability, good dispersion and low thermal expansion. © 2008 Wiley Periodicals, Inc. J Appl Polym Sci 109: 4112–4120, 2008

Key words: thermal properties; nanocomposites; surfactants; polyester; clay

INTRODUCTION

Polymer/clay nanocomposites have attracted great interest in industry in past decade, because their specifically improved properties make them as a valuable alternative to conventionally filled polymers.[1–5] To enhance the dispersion of clay in polymer matrix, the silicate particles were firstly modified with organic derivatives at surface through exchanged reaction, grafting reaction, or physical absorption.[6–8] The role of these organic surfactants is to reduce the surface energy of clay surface and to improve the interface interaction between clay and polymer.[9–11]

Subsequently, the clay particles with organic surfactants are directly introduced into the reaction systems at high temperature in some nanocomposite preparation methods. For example, in melting intercalation of PET/clay nanocomposites, the processing temperature is up to 270°C, and this temperature is so high that most commonly used organic surfactants, such as alkyl ammonium and amino silane coupling agents, have been decomposed.[12–14] Xie et al.[15] concluded that such decomposition of surfactants may alter the level of clay exfoliation and interfacial bonding, and then influence physical and mechanical properties of the final nanocomposites. Additionally, the decomposition of surfactants of modified clay may cause the polymer matrix degradation during preparation of nanocomposites, such as the extrusion of PET/organoclay[16] and the mixture of polycarbonate/organoclay.[17] Therefore, the thermal stability of organic component of the modified clay is one of the key issues in preparation of polymer/clay nanocomposites.

The objective of this study is to examine thermal stability of surfactants with amino and imido functional groups during the melt processing of PET/organic fibrous silicates composites. Thus, a new silane agent with imido functional group was fabricated successfully, which can be used to modify clay as surfactants. Specifically, thermal expansion and degradation is evaluated for nanocomposites made from different contents of organic clays. The mechanism of amino surfactants degradation was also investigated.

In this article, palygorskite clay was selected for covalently modification with the two alkoxy-silane surfactants. Palygorskite, also called attapulgite usually, is a kind of phyllosilicate characterized by a microfibrous morphology, high surface charge, and large specific surface area. Especially, the interaction between PT crystal particles is weaker than that of layered clays, such as montmorillonite, and these single crystals of PT can be exfoliated in aqueous medium through strong stirring or ultrasonic modification. Additionally, there are lots of hydroxyl functional groups at surface of PT single crystals, which is in favor of condensation reaction with alkoxyl-silane surfactants.[18–22] Compared with the layered structure of currently used montmorillonites, the

Correspondence to: Chuncheng Li (lizy@iccas.ac.cn).

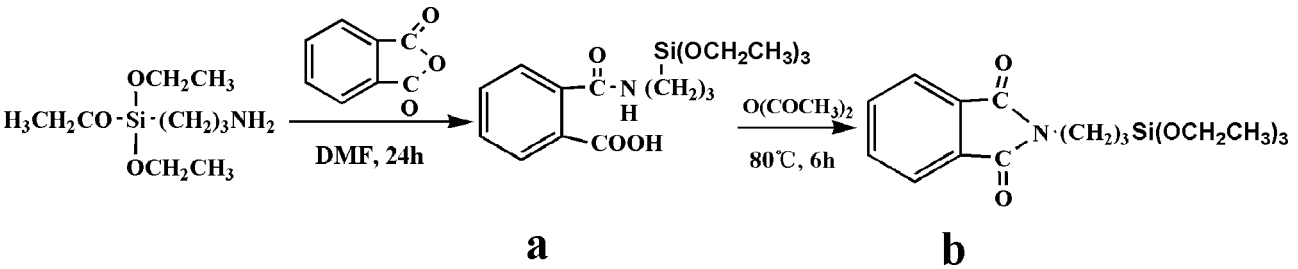

Figure 1 Scheme of synthetic procedures of imidosilane.

fibrous crystals of PT maybe provide low barrier effect on thermal degradation, which is benefited to the investigation on thermal stability of surfactants.

EXPERIMENTAL

Materials

The commercial PET materials were supplied from Beijing Yanshan Petrochemical (Beijing, China) Palygorskite (PT) clay (CEC = 25–30 mequiv/100 g, specific surface area 400–500 m^2/g) was obtained from Jiangsu Autobang International (Xuyi County, Jiangsu Province, People's Republic of China). Aminosilane coupling agent (γ-aminopropyltriethoxysilane, KH550) was a commercial product from Liaoyang Gaizhou Chemical (Liaoning Province, China). Phthalic anhydride, *N*,*N*-dimethylformamide (DMF), acetic anhydride, and pyridine were purchased from Beijing Chemical Reagents Company (Beijing, China).

Synthesis of imido surfactants

The synthetic procedures of imidosilane surfactant are generally shown in Figure 1. To the solution of phthalic anhydride (1 mmol) in DMF (20 mL), KH550 (1 mmol) was slowly added over a period of 30 min with stirring. The mixture was stirred at room temperature for 24 h, and then acetic anhydride (1.2 mmol) and a few drops of pyridine were introduced. After stirring for 6 h at 80°C, the liquid was removed under vacuum, and the residue was imidosilane as the yellow solid (10 g in 97% yield).

Preparation of organic PT

PT (10 g) was dispersed into 500 mL deionized water with a magnetic stirrer about 24 h at room temperature. Then the mixture was dispersed by the ultrasonic wave with an output of 200 W for 0.5 h. A predissolved KH550 solution (50 g H_2O, 50 g ethanol, 60 g acetic acid, and 5 g KH550) was slowly added to the clay suspension and stirred vigorously for 4 h at 90°C. The resultant mixture was filtered and washed with distilled water for six times to remove the residual acid and free coupling agents, as shown by universal indicator papers. The acquired clay was dried at 100°C, ground into powders. Imidosilane instead of KH550 was used to modify PT clay with the same procedures. The products were labeled as amino-PT and imido-PT, respectively.

Melt processing

The nanocomposites were fabricated via melt compounding of PET pellets and clay powders using a Haake twin screw extruder at 275°C with a screw speed 50 rpm. All the samples were dried in a vacuum over 90°C for 12 h before mixing. A wide range of PET/PT composites containing 0, 0.5, 1.0, and 3.0 wt % clay were prepared with pure PT, amino-PT and imido-PT, respectively.

Characterization

The dispersion morphology of fibrous clay particles in PET/clay nanocomposites was observed on a JEOL-100CX transmission electron microscope (TEM) with the ultrathin slices about 100 nm. The thermal decomposition studies were performed over a temperature range of 50–750°C using a Perkin–Elmer TGA-7 under nitrogen at heat rates of 20°C/min. All the TGA data reported here represent an average value of triplicate analysis, and the corresponding correlation coefficients were beyond 0.970. FTIR spectra were taken with a Perkin–Elmer FTIR system 2000 spectrometer for imidosilane and organic PT powders. The structure of imidosilane was proved by the ^1H NMR (300 MHz, $CDCl_3$): δ 7.73 (d, 2H, Ar—H); 7.60 (d, 2H, Ar—H); 3.73 (m, 6H, $—CH_2$); 2.90 (t, 2H, $—CH_2$); 1.76 (m, 2H, $—CH_2$); 1.26 (t, 2H, $—CH_2$); 0.68 (t, 9H, $—CH_3$). The coefficient of thermal expansion (CTE) and glass transition temperature (T_g) of certain samples were measured by thermal mechanical analysis (TMA) with a Perkin–Elmer TMA model 7 at a heating rate of 5°C/min from 0 to 190°C. The measurements were performed on samples taken from injection molded test specimens along the normal direction in dimension about 5 cm

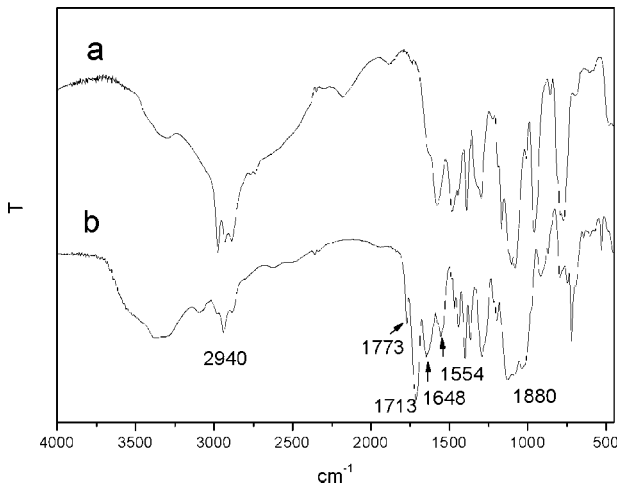

Figure 2 FTIR spectra of aminosaline (a) and imidosaline (b).

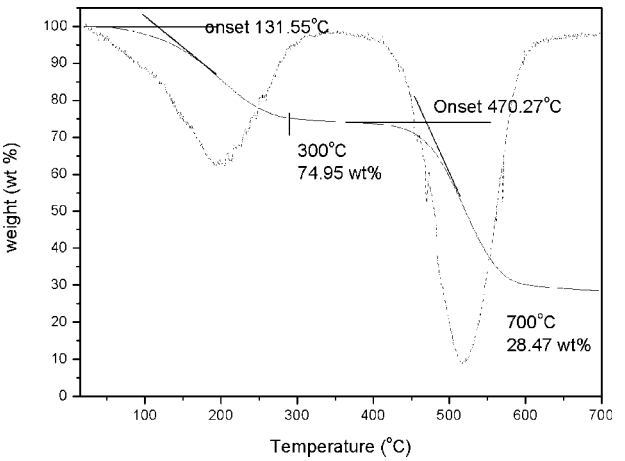

Figure 3 TGA (solid line) and DTG (dashed line) curves of imidosilane.

× 5 cm × 3.5 cm. To provide the needed minimum height, the thermal expansion was measured by stacking two specimens together. The intrinsic viscosity (IV) of all samples was measured at 25°C in an Ubbelohde viscometers with the mixture of 50/50 (wt/wt) phenol/1,1,2,2-tetrachloroethane as solvent.

RESULTS AND DISCUSSION

Characterization of surfactants

This study reports on the thermal stability of two surfactants with propyltriethoxysilane functional groups. These alkoxy-silane end groups can covalently bond onto the surface hydroxyl functional groups of PT by means of condensation reactions. It is an essential treatment to make the clay sufficiently organophilic to enable the organic polymer to insert between clay particles. Thus, the self-condensation reaction of ethoxylsilane groups should be avoided completely during the synthesis process of imidosilane from aminosilane and phthalic anhydride.

Firstly, the structure of imidosilane was analyzed by FTIR and ^{1}H NMR. From FTIR results [Fig. 2(b)], it is clear that the imido silane showed new absorptions bands at 1773 and 1713 cm^{-1} because of the stretching vibration of two C=O bonds in imido groups. The new absorption peaks at 1648 and 1554 cm^{-1} were assigned to the character of phenyl group. In their spectra, the strong absorption peaks of both surfactants at 1080 cm^{-1} are ascribed to Si—O stretching vibration, and the absorption peaks about 2940 cm^{-1} correspond to the stretching vibration of —CH_2. In the ^{1}H NMR spectrum of imidosilane, the peaks appeared at 3.7 and 7.7 ppm was assigned to —OCH_2 and phenyl, respectively. There is no peak at 9–13 ppm, which means no existence of —COOH as shown in Scheme 1(a) product. These results indicate that the synthesis of imidosilane was successful, and the nitrogen element in the imidosilane surfactant is in existence by means of imido group.

Figure 3 shows the TGA and the differential weight loss (DTG) curves obtained in a nitrogen atmosphere for imidosilane. The onset decomposition temperature (T_o) and peak decomposition temperature (T_{max}, the peak maximum temperature from DTG curves) are summarized in Table I. It is obvious that there are two major stages in decomposition of imidosilane between 100 and 700°C. Moreover, the two decomposition temperatures and the amount of weight loss in each stage are different. The first stage located from about 100–300°C, is accordant to the self-condensation reaction of the alkoxy-silane end groups. The weight loss of first stage is 25.05% from 100 to 300°C, corresponding to the theoretical loss of three ethoxyl groups in imidosilane (24.78%). The second stage (T_o = 470°C) is ascribed to the decomposition of phenyl, imido and propyl groups in imidosilane. The theoretical weight loss (53.57%) is higher than the data from experi-

TABLE I
Thermogravimetric Data of the Imidosilane

Decomposition stage	T_o (°C)	T_{max} (°C)	Experimental weight loss (%)	Theoretical weight loss (%)	Theoretical lost groups
First	132	197	25.05	24.78	Ethylic
Second	470	517	46.48	53.57	Phenyl, imido, propyl

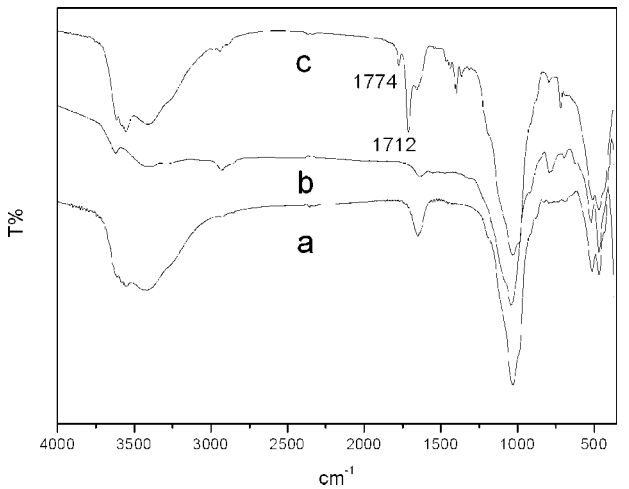

Figure 4 FTIR spectra of pure PT (a), amino-PT (b) and imido-PT (c).

ment (46.38%). The reason of this difference may be that the residual ashes up to 700°C are by means of not only Si—O bonds, but also Si—C bonds.

Characterization of organoclay

In the infrared spectra of pure PT and the two organo-PTs (Fig. 4), it is obvious that the PT modified with imidosilane showed new absorptions bands at 1774 and 1712 cm^{-1} (assigned to vibrations of C=O in imido groups). This indicates that imidosilane surfactants successfully grafted onto the surface of PT. In their spectra, the strong and wide absorption peaks of both organo-PT and pure PT in the higher wave number region at 3700–3200 cm^{-1} are ascribed to hydroxyl stretching vibration. The sharp absorption peaks about 1035 cm^{-1} correspond to the stretching vibration of Si—O bond.

TGA and DTG further confirm the presence of organic compound in the modified clay product, and demonstrate the thermal stability of surfactants at clay surface. As shown in Figure 5(a), for the unmodified PT, an initial weight loss at 212°C is because of the loss of hydration water. There was also another stage of decomposition at 476°C associated with the loss of co-ordination water in the aluminosilicate, and the final weak peak at 620°C was ascribed to the loss of water through dehydroxylation.[23] For PTs modified with aminosilane and imidosilane [Fig. 5(b,c)], it can be seen that the first two stages of weight losses located at the temperature similar to that of pure PT, and thermogravimetric data are shown in Table II. For amino-PT, the weight loss in second degradation stage from 350 to 550°C (4.51%) is near to that of pure PT (4.58%). However, the first weight loss from 160 to 290°C is 2.55%, which is higher than that of pure PT (1.71%). Based upon molecular structure and experimental results, Shah[11] and Xie[15] et al. suggested that thermal decomposition of alkyl ammonium surfactants at modified clay surface occurs mostly between 200 and 250°C with a Hoffmann elimination reaction. Therefore, it can be concluded that the decomposition of aminosilane surfactant occurred totally at the first weight loss stage (160–290°C), and the amount

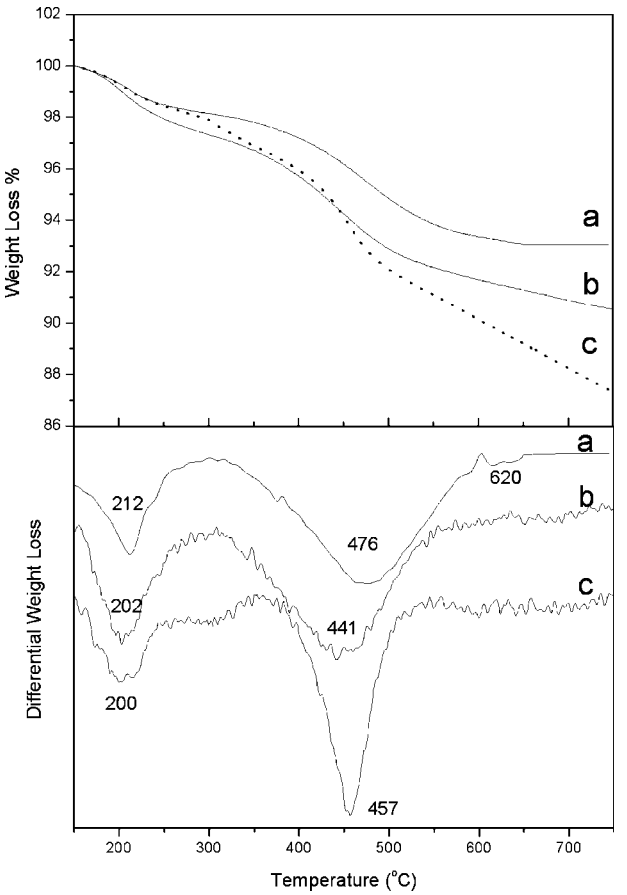

Figure 5 TGA and DTG cures for unmodified PT (a) and amino-PT (b) and imido-PT (c).

TABLE II
Thermogravimetric Data for Organic PTs and Pure PT

	First stage			Second stage		
Degradation stage	T_o (°C)	T_{max} (°C)	Loss (W) (%)	T_o (°C)	T_{max} (°C)	Loss (W) (%)
Pure PT	154	212	1.71	402	476	4.58
Amino-PT	170	202	2.55	385	441	4.51
Imido-PT	168	200	1.74	430	457	7.29

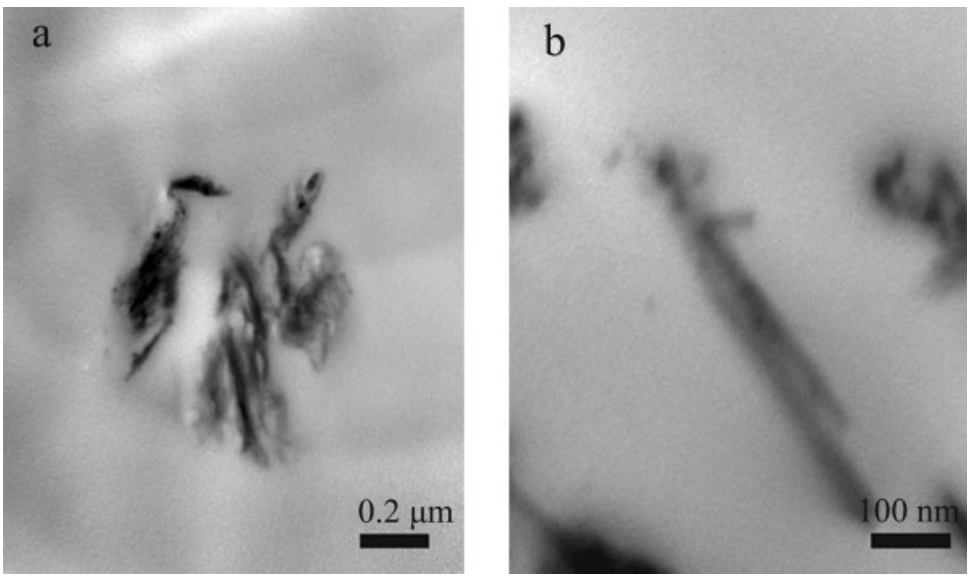

Figure 6 TEM images of PET/amino-PT (a) and PET/imido-PT (b) with 3 wt % loading.

of lost organic derivatives was 0.84% from the difference of TGA data between amino-PT and pure PT (2.55–1.71%). It also indicates that there are 0.84 g aminopropyl groups of aminosilane per 100 g of amino-PT.

Different to amino-PT, at the first weight loss stage, the imido-PT has the similar loss weight data (1.74%) with that of pure PT (1.71%). Whereas at the second degradation stage, the loss weight datum of imido-PT (7.29%) is higher than that of pure PT (4.58%) and amino-PT (4.51%), which means that the decomposition of imido groups happens at the second degradation stage. As shown in Table II, the actual content of organic surfactans of imido-PT (phthalimidopropyl groups) was determined based on the different weight loss at the second degradation stage, which was about 2.71% (the difference between 7.29% of imido-PT and 4.58% of pure PT). According to the molecular weight of these two grafted groups of surfactants (aminopropyl and phthalimidopropyl groups, 58 g/mol and 188 g/mol), the density of organic substance in modified PT can be calculated out as: 14.48 and 14.41 mequiv per 100 g of amino-PT and imido-PT, respectively. These two data are in good agreement, which means that the alkoxy-silane groups of both surfactants were successfully bonded onto the surface hydroxyl functional groups of PT with the same quantities of reactive sites.

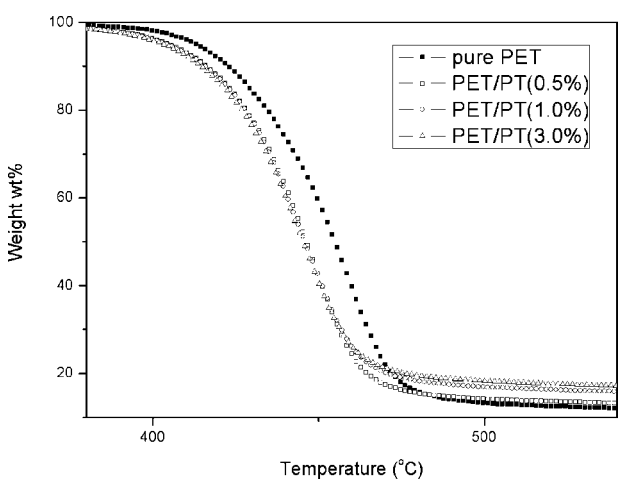

Figure 7 TGA cures of virgin PET and PET/pure PT composites with different loads.

In conclusion, the organic constitution in amino-PT begins to decompose (T_o in Table II) at first weight loss stages between 170 and 250°C, but the imido-PT starts degradation over 430°C at second weight loss stages. It means that imido-PT presents excellently higher thermal stability than that of amino-PT. This result corresponds to previous work with various ammonium cations in the montmorillonite that the initial degradation of the surfactants follows a Hofmann elimination reaction. Xie et al.[15,24,25] suggested that the small amount of organic salt associated to the surface of aluminosilicate, and not confined in the interlamellar region, is released firstly, leading a weight loss at 170–400°C. They argued that the architecture (trimethyl and dimethyl silane), chain length, surfactant mixture, exchanged ratio, or preconditioning (washing) does not alter the initial onset temperatures.

According to the structure of PT clay, the surfactants are always located at single rod-liked crystal surface because of the weak interaction between PT crystal particles. Therefore, compared with the surfactants in the interlamella regions of montmorillonites, the aminosilane surfactants at PT surface begin

TABLE III
Thermogravimetric Data for PET and PET/PT in Nitrogen at the Heating Rate of 20°C/min

Samples	T_o (°C)	T_{50} (°C)	T_{max} (°C)	Residue at 540°C (wt %)
PET	413	455	457	12.14
PET/PT (0.5%)	404	446	447	13.27
PET/PT (1.0%)	404	446	440	15.90
PET/PT (3.0%)	403	445	448	17.21
PET/amino-PT (3.0%)	402	443	446	14.56
PET/imido-PT (3.0%)	414	456	458	16.45

to degrade easily, even at 170°C. However, if the amino groups were replaced by imido groups in silane surfactants, the onset decomposition temperature increased greatly. It is possible that the imido groups with high thermal stability are difficult to decompose, compared with the amino groups. Thus, the low stability of the amino-PT should be attributed to the thermal instability of the nitrogen–carbon bond, leading to the more facile loss of organic substance at PT surface.

Characterization of PET/PT composites

It is generally accepted that the surface properties of organoclay is crucial to the dispersion of polymer/clay nanocomposites. The direct observation of dispersion of fibrous silicate in polymer matrix was obtained by means of TEM, as shown in Figure 6, which was for the two series of PET composites with 3 wt % loading of amino-PT and imido-PT. It can be seen that there is a marked difference in the dispersion morphology in the two specimens. For PET/amino-PT in Figure 6(a), there are obvious aggregations with the size over 1 μm. However, in Figure 6(b) of PET/imido-PT composites, it was possible to observe single fibrous silicate crystals with a length over 500 nm and a diameter about 50 nm. Although PET/imido-PT hybrid materials should hardly be called as ''exfoliated nanocomposites,'' their dispersion of clay particles was obviously better than that of PET/amino-PT composites. According to the TGA curves in Figure 5, the amino-PT starts to decompose at 170°C, whereas imido-PT retains superior thermal stability below 430°C. Therefore, under the PET processing temperature about 250–270°C, for PET/amino-PT, the surface decomposition of amino-PT could result into the aggregations of silicates particles in PET matrix once again. Compared with PET/amino-PT, PET/imido-PT has the enhanced thermal stability of organo-PT, which is in favor of dispersion of nanocomposites.

The thermal degradation of PET has been studied extensively under a variety of conditions. Generally, a common agreement was proposed that PET degrades with random chain scission at the ester linkages, and the methylene group is believed to be the principal point of weakness.[26–28] As a result, the melt temperature, melt residence time, moisture and the additive fillers have been found to affect the thermal stability of PET strongly. To study the role of surfactants in PET chains degradation, it is necessary to examine the effect of additive fillers (pure PT clay in PET/PT composites) on thermal degradation with the absence of surfactants.

The TGA curves of unmodified PT/PET composites are depicted in Figure 7. T_o, T_{max} and T_{50} (the mid-point temperature of degradation occurs), as well as the fraction of material that is not volatile at 540°C, are summarized in Table III. Compared with virgin PET, the thermal stability of these composites appears to decrease much with the addition of PT clay, even with 0.5% content of PT. For instance, T_{50} of virgin PET is about 10°C higher than that of PET composite with 3 wt % PT. Similar trends have been reported by Matayabas et al. for melt processed PET-organoclay nanocomposites: the addition of clay accelerates the degradation of polyester chains.[16] These curves of composites with the different clay contents almost superposed together, which indicates that the addition of PT clay affects the thermal stability of PET observably, and the degradation behaviors hardly depend on the amount of additive

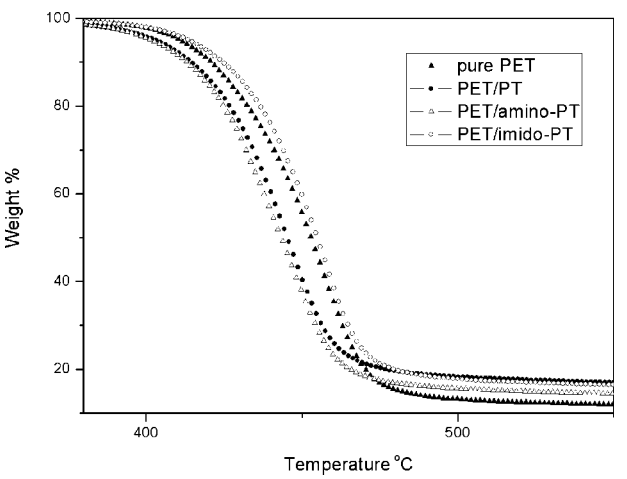

Figure 8 TGA curves of pure PET and PET composites with 3 wt % load of clay.

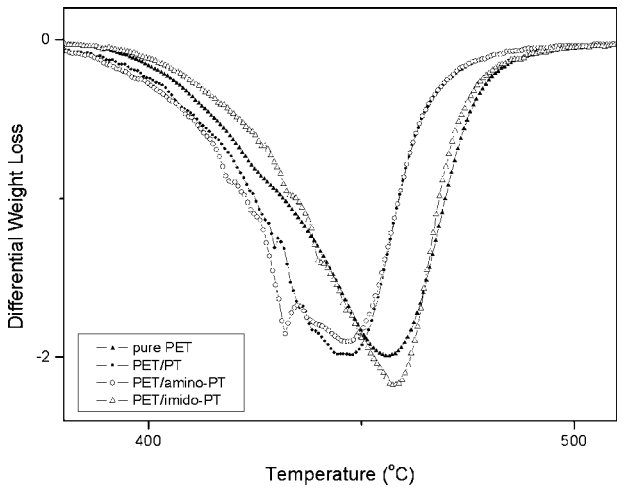

Figure 9 DTG curves of PET and composites with 3 wt % load of clay.

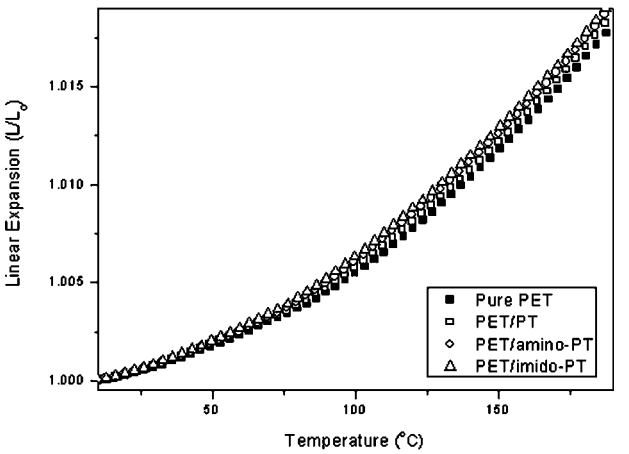

Figure 10 TMA curves of pure PET and PET composites with 3 wt % loading of clay.

fillers. This degradation should be due to the hydration water in clay, which lost at the temperature of 212°C as shown in Figure 5(a). Because the small amount of moisture has marked effect on thermal stability of PET, the sufficient drying pretreatment of clay fillers was necessary before melt process.

The thermal stability of PET composites containing 3 wt % clays with different surfactants was investigated by TGA, shown in Figure 8 and Table III. It is apparent that the addition of pure PT and amino-PT facilitated the decomposition of polyester chains, but the addition of imido-PT enhanced the thermal stability of PET composites. For examples, T_o of virgin PET, PET/pure PT, PET/amino-PT and PET/imido-PT are about 413, 403, 402 and 414°C, respectively. The observed stabilizing effect of imodo-PT on thermal stability of PET nanocomposite is attributed to a shielding effect of clay particles in polymer matrix because of the good thermal stability of imidosilane surfactants. These dispersive clay particles likely block active sites in polymer chains that would reduce the mass transport rates during the degradation process. On the other hand, the decomposition of aminosilane surfactant at the PET processing temperature (275°C) makes the clay particles agglomerated together again, which reduces the shielding effect and accelerates the degradation of PET composites. Furthermore, according to the literatures of Xie et al.,[15,24,25] a Hoffman elimination reaction for alkyl ammonium modified clay may occur at the initial degradation with the formation of amines, water and other products. Obviously, those decomposition products of aminosilane surfactants can accelerate the degradation of PET chains. Therefore, the thermal stability of PET/amino-PT is lower than these of others. These results indicate that the thermal stability and degradation behavior of those composites are influenced by the surfactants types, especially, the thermal stability of surfactants.

In Figure 9, DTG curves of PET and PET-clay composites were calculated out from thermogravimetric data in Figure 8. Obviously, T_{max} of PET/imido-PT is higher than that of others, and T_{max} of PET/amino-PT is lowest (data in Table III). Otherwise, a small peak appears at 432°C in the curve of PET/amino-PT nanocomposite in Figure 9, which means that degradation behavior of composite suddenly accelerated at this temperature. Similar trends have been found in the curves of PET/PT and imido-PT composites except pure PET. According to the results in Figure 5, approximately at 430°C, the co-ordination water in silicate began to release out, and this small quantity of water can seriously affect degradation behaviors of PET matrix. Therefore, this acceleration of degradation in Figure 9 should be

TABLE IV
TMA Data of Pure PET and PET Composites

Samples	PET	PET/PT	PET/amino-PT	PET/imido-PT		
Clay %	0	3 wt %	3 wt %	0.5 wt %	1 wt %	3 wt %
T_g (°C)	96.1	86.9	84.0	86.5	83.2	81.8
CTE$_g$ ($\times 10^{-6}$) (°C)	56.80	57.48	59.53	59.94	60.32	62.02
CTE$_r$ ($\times 10^{-6}$) (°C)	161.5	154.4	152.1	158.5	156.2	151.3

attributed to the lost of co-ordination water in PET-clay nanocomposites.

The TMA experaments were performed on PET and PET/PT composites to determine their thermo-mechanical behavior. Figure 10 shows the measured relative linear dimension (L/L_o) as a function of temperature for pure PET, PET/PT, PET/amino-PT and PET/imido-PT from 0 to 190°C. Linear thermal expansion coefficients, CTE_g below T_g from 30 to 60°C, and CTE_r above T_g from 130 to 180°C, were calculated from the slopes of the lines. As shown in Figure 10 and Table IV, the CTE_r decreased with the dispersion of nanocomposites. For example, the CTE_r of PET/imido-PT with good dispersion is 151.3, which was lower than that of PET/PT, PET/amino-PT and pure PET. It means that, over T_g, the polymer chains' movement activity was restricted by dispersion of individual silicate particles. Good dispersion provides a higher level of polymer constraint when compared with the worse dispersion because of the larger number of particles and higher aspect ratios that result from an increased amount of exposed silicate surface effect contact with the polymer. Therefore, better exfoliation should lead to less thermal expansion over T_g during heating process. However, below T_g, the polymer chains were forbidden to move freely, and the dispersion of individual particles can reduce the limit of chains' movement because of the extreme differences in stiffness and thermal expansion between the polymer matrix and filler. As a result, CTE_g increased with the dispersion of nanocomposites.

The CTE_r, CTE_g and T_g for the PET/imido nanocomposites as a function of silicate content were shown in Figure 11. The CTE_r and T_g were decreased as the PT loading increased for nanocomposites, which is according with the previous reports about nylon6/clay nanocomposites[29] and polypropylene nanocomposites.[30] For PET nanocomposites

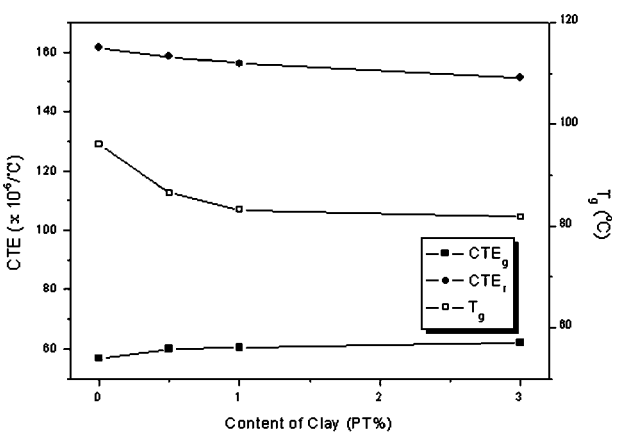

Figure 11 Linear thermal expansion coefficient and T_g of specimens with various loading of silicates.

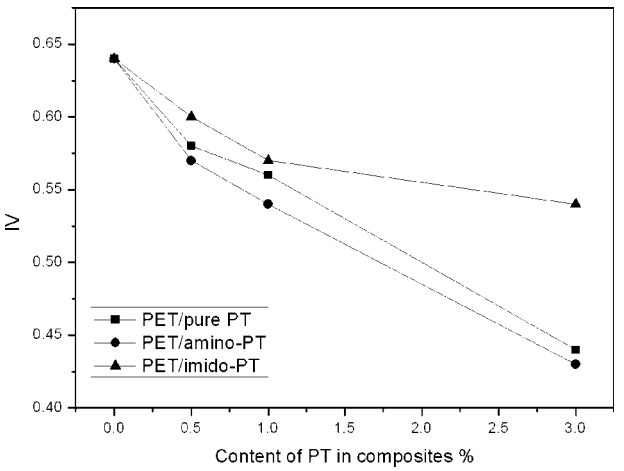

Figure 12 Intrinsic viscosity (IV) of PET composites with different surfactants.

containing 3 wt % imido-PT, the CTE_r decreased nearly to 10% when compared with that of pure PET. This reduce is due to the constraint effect caused by clay particles in polymer chains movement. However, the CTE_g increased linearly with the content of clay, which should was ascribed that the exfoliated clay particles hindered the freezing behavior of polymer chains and enhanced the chains movement activity.

The IV breakdown of PET composites with different contents of pure PT, amino-PT and imido-PT via melt extrusion is shown in Figure 12. Compared with PET/pure PT, the thermal stability of PET/imido-PT is higher and that of PET/amino-PT is lower. It corresponds to the results in TGA (Figs. 5, 8 and 9). Otherwise, it appears that the molecular weight of these composites is decreased as the increasing clay content, which is consistent with the reports of Matayabas et al.[16]

CONCLUSIONS

In this article, a new silane agent with imido functional groups was synthesized to modify PT clay as organic surfactants. Compared with the amino silane surfactants, the imido silane shows high thermal stability with two major decomposition stages of different functional groups. As a result, the organoclay modified by imido silane surfactants has higher thermal stability than that of amino-PT. After melt processing, thermal stability of these surfactants in organoclays has significant effect on the properties of PET/clay composites, although the addition of pure clay can affect degradation behaviors of PET matrix also. The amino groups in surfactants begin to decompose at 170°C, under the PET melt processing temperature (about 270°C), they release some decomposition products and decrease the thermal

stability of PET/amino-PT composites greatly. However, PET/imido-PT nanocomposites have high thermal stability and excellent dispersion because of the good thermal stability of imidosilane surfactants. Especially, the high remained intrinsic viscosity after melting process was in favor of the practical application of facilely degradable polyesters. The low thermal expansion was benefited to reduce the thermal shrinkage and widen the PET application such as fiber, film and bottle with steady dimension.

References

1. Okada, A.; Kawasumi, M.; Kurauchi, T.; Kamigaito, O. Polm Prepr 1987, 28, 447.
2. Giannelis, E. P. Adv Mater 1996, 8, 29.
3. Ray, S. S.; Okamoto, M. Prog Polym Sci 2003, 28, 1539.
4. Utracki, L. A.; Sepehr, M.; Boccaleri, E. Polym Adv Technol 2007, 18, 1.
5. Okada, A.; Usuki, A. Macromol Mater Eng 2007, 291, 1449.
6. Guan, G.; Li, C.; Zhang, D. J Appl Polym Sci 2005, 95, 1443.
7. Xi, Y.; Frost, R. L.; He, H.; Kloprogge, T.; Brostrom, T. Langmuir 2005, 21, 8675.
8. Wheeler, P. A.; Wang, J.; Baker, J.; Mathias, L. J. Chem Mater 2005, 17, 3012.
9. Fornes, T. D.; Hunter, D. L.; Paul, D. R. Macromolecules 2004, 37, 1793.
10. Dharaiya, D.; Jana, S. C. Polymer 2005, 46, 10139.
11. Shah, R. K.; Paul, D. R. Polymer 2006, 47, 4075.
12. Su, S.; Wilkie, C. A. Polym Degrad Stab 2004, 83, 347.
13. Awad, W. H.; Gilman, J. W.; Nyden, M.; Harris, R. H. J.; Sotto, T. E.; Callahan, J.; Trulove, P. C.; Delong, H. C.; Fox, D. M. Thermochim Acta 2004, 409, 3.
14. He H.; Duchet J.; Galy J.; Gérard J. F. J Colliod Interface Sci 2006, 295, 202.
15. Xie, W.; Cao, Z.; Pan, W.; Hunter, D.; Singh, A.; Vaia, R. Chem Mater 2001, 13, 2979.
16. Matayabas, J. J.; Turner, S. R. In Polymer-clay nanocomposites; Pinnavaia, T. J.; Beall, G. W. Eds.; Wiley: New York, 2000; p 207.
17. Yoon, P. J.; Hunter, D. L.; Paul, D. R. Polymer 2003, 44, 5341.
18. Bradley, W. F. Am Miner 1940, 25, 405.
19. Cao, E.; Bryant, R.; Williams, D. J. A. J Colloid Interface Sci 1996, 179, 143.
20. Yuan, X.; Li, C.; Guan, G.; Liu, X.; Xiao, Y.; Zhang, D. J Appl Polym Sci 2007, 103, 1279.
21. Shen, L.; Lin, Y.; Du, Q.; Zhong, W.; Yang, Y. Polymer 2005, 46, 5758.
22. Wang, L.; Sheng, J. Polymer 2005, 46, 6243.
23. Frost, R.; Ding, Z. Thermochim Acta 2003, 397, 119.
24. Zhu, J.; Morgan, A. B.; Lamelas, F. J.; Wilkie, C. A. Chem Mater 2001, 13, 3774.
25. Xie, W.; Cao, Z.; Liu, K.; Pan, W.; Vaia, R.; Hunter, D.; Singh, A. Thermochim Acta 2001, 367, 2979.
26. Pohl, H. A. J Am Chem Soc 1951, 73, 5660.
27. Zimmerman, H.; Kim, N. T.; Polym Eng Sci 1980, 20, 680.
28. Jabarin, S. A.; Lofcren, E. A. Polym Eng Sci 1984, 24, 1056.
29. Yoon, P. J.; Fornes, T. D.; Paul, D. R. Polymer 2002, 43, 6727.
30. Lee, H.; Fasulo, P. D.; Rodgers, W. R.; Paul, D. R. Polymer 2006, 47, 3528.